THE SEVENTH ASIAN CONGRESS OF FLUID DYNAMICS
DEC 8-12, 1997, MADRAS, INDIA

VELOCITY FIELD MEASUREMENTS IN 3D ROTOR FLOWS

UC Reddy and NM Komerath
School of Aerospace Engineering
Georgia Institute of Technology
Atlanta, GA 30332-0150

ABSTRACT This research aims to measure four-dimensional, spatio-temporal velocity fields in unsteady periodic flows, such as those around rotorcraft. Periodic planar velocity fields at several slices of the flowfield are used to compute the component normal to the planes. The flow being incompressible, satisfying the continuity equation is sufficient. The velocity field reconstruction technique is validated against the Bödewadt-Nydahl solution for viscous rotating flow above a wall. The technique is shown to be robust to 15% band-limited white noise in boundary and other planes. The high Reynolds-number velocity field between a 2-bladed rotor and a wing in a large wind tunnel is captured using Spatial Correlation Velocimetry at video rate using pulsed laser sheet images in 27 planes across the rotor wake. The planar velocity data correlates well with previous flow imaging and single-point laser velocimetry results.

1. INTRODUCTION

While high-speed flows and the resolution of fine scales of motion have been intensively studied in aerospace research for obvious reasons, it remains surprisingly difficult to measure slow-moving flows over large areas and volumes. Applications requiring such a capability occur in flows around V/STOL aircraft in ground effect, landing pad turbulence in urban areas, and circulation in cabins and test chambers. Such flows involve large-amplitude fluctuations, and flow reversal of all 3 components, and sharp spatial gradients. The problem is approached from the perspective of tomographic reconstruction, specialized to vector fields. The out-of-plane velocity component requires an additional equation beyond the stacking of slices which suffices for scalar fields. The slices themselves require simultaneous data in multiple planes. Here we take advantage of the periodicity of the rotor and rotor/body flowfields investigated to ensemble-average phase-resolved data taken from different rotor cycles. The measurement of multiple planes of two component velocity fields using a cross-correlation method (SCV) was used as a precursor to the complete 3D three component velocity field measurement. The additional equation needed for the 3rd component is provided by mass conservation in incompressible flow.

2. SPATIAL CORRELATION VELOCIMETRY

In large flowfields such as those around rotorcraft, it is extremely expensive to conduct imaging with sufficient resolution for Particle Image Velocimetry (PIV). This problem was solved using the Spatial Correlation Velocimetry (SCV) technique [1]. Patterns of inhomogeneities are directly cross-correlated between sub-images using the efficient frequency-domain algorithm enabled by the Wiener-Khintchine theorem [2], to extract the large-scale velocity field. It can be easily shown that auto-correlation based PIV is a subset of this technique.

The implementation in rotorcraft flows is as follows : A light sheet illuminates a thin slice of the flow field. Intensified cameras are used to image seeding moving through this light sheet. Two short-exposure images separated by a small, controllable time are digitized from the two cameras, each of which runs at video rate. The images are sub-divided into small sub-image arrays and a spatial cross-correlation is performed on corresponding sub-images. The displacement of the cross-

correlation peak from the origin, divided by time between images, gives the scaled velocity vector with no directional ambiguity.

3. 3D VELOCITY FIELD RECONSTRUCTION

A second order finite difference scheme is used to compute the differential change in the third component of velocity between successive parallel 2D data planes. One sided difference is used for the edge points and central difference for the interior points. These differentials are numerically integrated to obtain the third component, satisfying the continuity equation. The solver steps across the flow, starting from two boundary planes where the component of velocity normal to the plane is known (usually zero or constant), so that all components and their gradients can be specified in these planes. In the wind tunnel the boundary conditions are provided by the freestream (uniform flow) or walls (zero normal velocity).

A test case of rotating flow interacting with a stationary ground was chosen to validate the third velocity component (TVC) algorithm. Although the axial flow is in the opposite direction, this flow contains some of the elements of the flow around a helicopter in ground effect. The strong gradients associated with the tip vortices are absent in this problem. However, we do have a swirling flow, a rapidly varying axial velocity profile and a large radial variation near the ground plane. Fluid at large distances from the ground is in equilibrium under the influence of centrifugal force and radial pressure gradient and is assumed to rotate with constant angular velocity. In the boundary layer, viscous forces attenuate the outward centrifugal force and there is a radial inflow as shown in the schematic in Fig. 1. The upward secondary flow ensures continuity. The exact solution to the Navier-Stokes equations in cylindrical coordinates for this problem was found by U.T. Bödewadt [3] using a power series expansion. J.E. Nydahl's [4] corrected solution was used to generate the 2D velocity field in several parallel planes and validate the results for the third component. Slices of this 3D vector field near the ground and in the farfield are shown in Fig. 2.

3.1 Numerical Simulation: The exact solution was used to generate 27 slices of 2D velocity data (41 x 31 grid) parallel to the ground. The farfield angular velocity was specified at 1050 RPM. The axial velocity depends only on the distance from the ground. Hence the plots shown for the reconstructed axial velocity are one dimensional - the x-axis is height from the ground and the y-axis is the non-dimensional axial velocity averaged over all grid points in a plane parallel to the ground.

To simulate experimental data, white-noise of amplitude up to 25% of the exact values was added to the inplane components throughout the measurement volume and to all three components at the boundary planes. Measurement noise was increased from 0% in steps of 5% and resulting axial velocity profile compared to the Bödewadt-Nydahl solution. When the two boundary planes are in the farfield, the results match the exact solution closely (up to 25% noise) except in the region of sharp gradient near the ground. However, with ground boundary planes there is noticeable deviation from exact solution. This indicates that steep gradients near the boundary planes lead to errors in reconstruction. Figure 3 shows the axial velocity profiles with 25% measurement noise with both farfield and ground boundary planes. It is seen that adding as much as 25% random measurement noise still gives a good reconstruction of the out-of-plane component when boundary conditions are suitable.

4. DESCRIPTION OF EXPERIMENT

Figure 4 shows a full-span NACA0021 wing with 400 mm chord at 0° angle of attack, mounted below a 914 mm diameter, 2-bladed teetering rotor in the 2.7m x 2.1m windtunnel. The rotor hub is at mid span, 127 mm upstream of the wing leading edge. A wing has a cambered trailing edge flap of 125 mm chord. The tunnel speed of 3.77m/s and rotor speed of 1050 RPM gave an advance ratio of 0.075. A dual-camera system, with externally controlled shutter delay, captures images from the pulsed copper vapor laser sheet, operating at 5994 pulses/sec. Shutter exposure is set to capture just one pulse in each image. The light sheet is stepped normal to itself in steps of 5 cm covering the entire rotor wake and extending to the tunnel wall on the retreating blade side (RBS).

The measurement area is about 650 mm x 650 mm. The visualization is recorded for 3 different delays between the camera shutters to capture a wider range of flow speeds.

5. RESULTS AND DISCUSSION

The downstream half of the rotor wake region was measured. Several vector fields were phase-sorted and ensemble averaged at each location. Each second of video recording yielded 60 different images of the flow. Typically 10 sec. movie clips were analyzed at each location i.e. 600 vector fields. The delay between camera shutters is the temporal resolution of the velocity measurement. The vector fields obtained are therefore associated with the middle of the delay between the two shutters.

Analysis of earlier flow visualization data revealed that two different vortex trajectories exist [5]. These trajectories repeat each rotor revolution and are traced to the different blades of the two bladed rotor system. This divergence of vortex trajectories is reflected in the vorticity contours computed from planar velocity fields measured using SCV. Figure 5 shows the 2D ensemble-averaged velocity field overlaid on vorticity contours at a chordwise vertical plane at $y/R = -0.22$ for a rotor azimuth of 174° (0° azimuth is with blades aligned with the freestream direction). The flow turning visible near the leading edge of the wing progresses to reversed flow at later azimuths and indicates vortex interaction. Regions of comparable vorticity are also seen upstream of the trailing edge. This indicates two vortex trails impinging on the wing - one that goes over the leading edge and the other that goes over the wing surface.

Due to vortex interactions the flow pattern at a given point repeats only once per rotor revolution. Ensemble averaged traces of vertical and streamwise velocity components at selected points in the flow clearly indicate a once-per-rev variation. The variation is quite consistent, even though the individual values are picked off different vector fields. However, there is more scatter from point to point than we see in ensemble-averaged LDV data [6]: this is not surprising, given that only 25 values are averaged in each azimuth interval compared to an average of 300 points in a typical LDV azimuthal bin.

6. CONCLUSIONS

An integrated capability is presented to quantify instantaneous 3D incompressible periodic velocity fields over large volumes. A second order finite difference scheme with two boundary planes specified is sufficient for a reliable reconstruction of the third velocity component from closely spaced planes of 2-D velocity data. The robustness of the TVC solver to random experimental noise has been demonstrated.

The application of the technique to a rotor-wake interaction experiment in a large wind tunnel has been described. Phase-resolved, ensemble-averaged velocity fields have been acquired in a 3D periodic rotor wake over a wing. The planar velocity data are consistent enough to compute vorticity contours which show the expected transient flow features. The divergence of the vortex trajectories, and their flowfield effects, are clearly seen.

ACKNOWLEDGMENTS

This work was performed under the Rotorcraft Center of Excellence, funded by the Army Research Office. Dr. T.L. Doligalski is the technical monitor.

REFERENCES

[1] Komerath, N.M., Fawcett, P.A., "Spatial Cross-Correlation Velocimeter", U.S. Patent 5,249,238, Sept. 1993.

[2] Pierce, A.D., "Acoustics: An Introduction to Its Physical Principles and Applications", McGraw-Hill, 1981, pp. 86-88.

[3] Bödewadt, U.T., “Die Drehströmung über festem Grund”, ZAMM 20, 241-253 (1940).

[4] Nydahl, J.E., ”Heat transfer for the Bödewadt problem”, Dissertation, Colorado State University, Fort Collins, Colorado, 1971.

[5] Funk, R.B., Crawford, B.G., Reddy, U.C., “Vortex Induced Transient Separation on a Lifting Surface”, 32nd Aerospace Sciences Meeting & Exhibit, Reno, Nevada, Jan. 1994.
[6] Funk, R.B., Komerath, N.M., “Proceedings of the 51st Annual AHS Forum and Technology Display”, Fort Worth, Texas, May 1995.

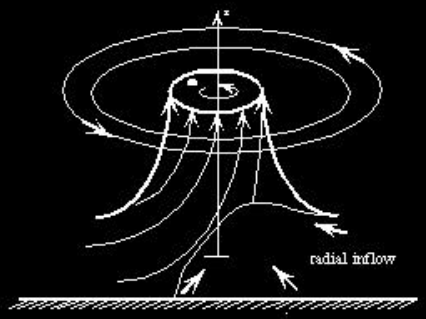

Fig. 1. Rotating flow near ground

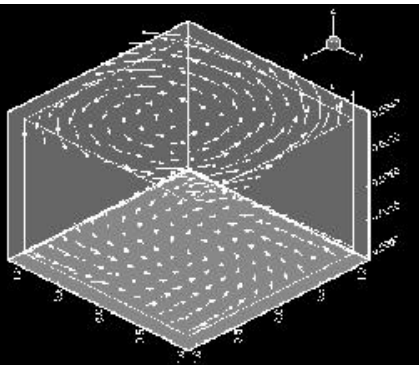

Fig. 2. The Bödewadt-Nydahl Solution

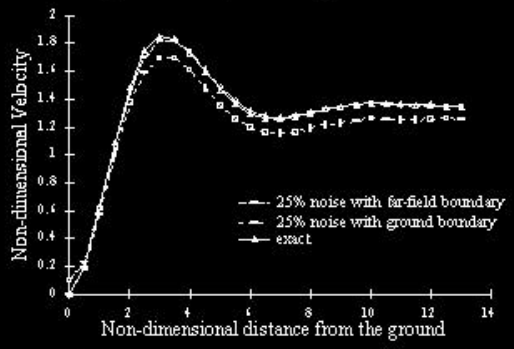

Fig. 3 Exact andcalculated axial velocity profiles (with random noise added)

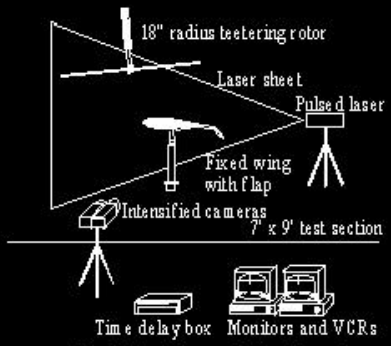

Fig. 4 Experimental Configuration

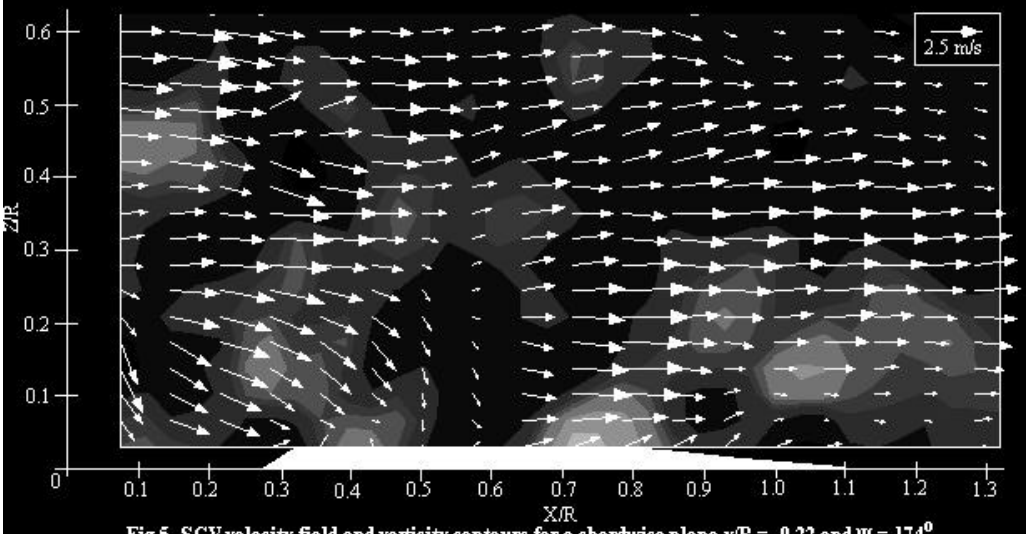

Fig.5. SCV velocity field and vorticity contours for a chordwise plane y/R = -0.22 and Ψ = 174^{0} (Rotor TPP at Z/R = 0.92)